ASTFE
American Society
of Thermal and Fluids Engineers

9th Thermal and Fluids Engineering Conference (TFEC)
April, 2024
Partially Online Virtual and at Oregon State University, Corvallis, OR

TFEC-2024-50713

IMPROVING HEAT FLUX MEASUREMENT ACCURACY IN SOLAR FARM ENVIRONMENTAL STUDIES: A CORRECTIVE EQUATION APPROACH

Daniel Trevor Cannon[1] Ahmad Vasel-Be-Hagh[2,*]

[1]Mechanical Engineering Department, Tennessee Tech University, TN, 38501, USA
[2]Department of Mechanical Engineering, University of South Florida, FL, 33620, USA

ABSTRACT

The environmental impact of solar farms, including photovoltaic and concentrated systems, has been the subject of extensive research. One critical parameter examined in these studies is total surface heat flux, which includes the summation of radiation and convectionat the panel's surface. A widely adopted method for measuring surface heat flux involves using direct-contact surface heat flux sensors. However, many of these studies overlook the radiation induced errors that lead to readings that underestimate the actual heat transfer. This problem cannot be simply addressed by adding radiation shielding to the sensor because doing so would block radiation heat flux, which is the actual source of heat one would want to measure. Hence, we designed this study to deliver a corrective equation to estimate and rectify this measurement error. Using data obtained from an experimental setup placed in the field, We computed how much an unshielded heat flux sensor underestimates the total heat flux. Using linear curve-fitting, we developed an equation that best describes the relation between this error and the incoming long-wave radiation.

KEY WORDS: solar; filed measurements; irradiance; heat flux

1. INTRODUCTION

The contribution of solar energy to global electricity generation is increasing, marked by the addition of massive solar facilities like the Bhadla Solar Park, which has 10 million Photovoltaic (PV) panels across 14,000 acres. Such expansive arrays of dark surfaces alter radiation. They also change convection as they add to surface roughness. The change in surface heat flux can potentially alter the atmospheric properties within the boundary layer. This motivated our team to investigate the impact of these solar plants on the atmospheric boundary layer, particularly the viscous sublayer. Our investigations include direct measurements of surface heat flux and temperature. In addition to such environmental studies, measuring solar panels' surface temperature and heat flux has engineering applications as they directly impact the plant's power performance. Hence, assessing solar panels' surface heat flux and temperature within utility-scale solar plants' supervisory control and data acquisition (SCADA) systems is common [1]. The panel's surface temperature and flux are generally measured via direct-contact surface heat flux and temperature sensors. These thin sensors attach to the panel as they are exposed to the air on the opposite side. Consequently, one side reflects the panel's temperature, while the other is intended to correspond to the air temperature. This temperature difference between both surfaces is the basis for estimating the heat flux. However, the temperature of the sensor's surface facing the air would be much larger than that of the air due to the absorption of radiative heat, leading to a smaller temperature difference between the two surfaces of the sensor. This causes an undermeasurement of heat flux. Conversely, as sensors are typically brighter than the dark PV panels, aimed at minimizing the mentioned radiation-induced error, the total irradiance absorbed at the sensor's location is anticipated to be lower than at all other locations. Hence, the PV panel's surface temperature would be relatively lower at the sensor's location. This increases the temperature difference between the sensor's two sides, increasing the measured heat

*Corresponding Ahmad Vasel-Be-Hagh: vaselbehagh@usf.edu

(a)

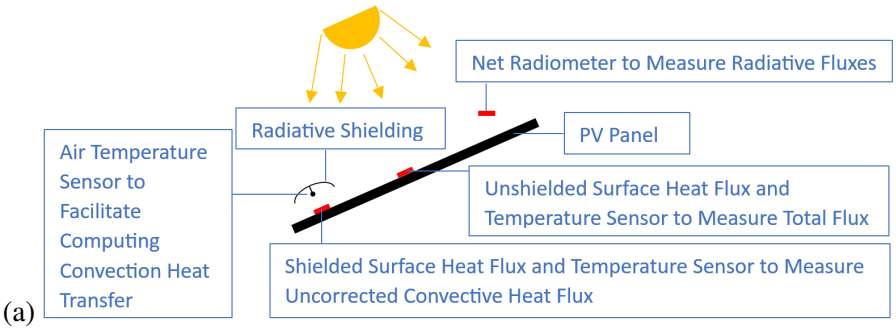

Fig. 1 The experimental setup.

Table 1 Used instruments' uncertainties. All sensors are analog; hence, their resolution is dictated by the 18-bit data logger's resolution.

Sensor	Measured Parameter	Calibration	Resolution	Combined	Total
Hukseflux FHF04 (50x50 mm²)	Panel's front and back surface temperature	5%	1 C	Measurement Dependent	Measurement Dependent
	Panel's front and back surface heat flux	5%	0.025 W/m²	Measurement Dependent	Measurement Dependent
Apogee SL-510-SS and SL-610-SS Pyrgeometer	Long-wave radiation coming off or going into the sky	5%	0.008 W/m²	Measurement Dependent	Measurement Dependent
Apogee SP-510-S$ and SP-610-S$ Pyranometer	Short-wave radiation coming off or going into the sky	5%	0.006 W/m²	Measurement Dependent	Measurement Dependent
Omega EWSA-PT1000	Air temperature above the panels	0.15 + 0.002T C	0.1 C	Measurement Dependent	Measurement Dependent

flux. This increase would, to some extent, offset the sensor's underestimation described above. This research aims to formulate an empirical equation that addresses the impact of the above-described radiation-induced errors. This equation will enable researchers to use a direct contact heat flux sensor without any shielding to measure the total surface heat flux accurately. Researchers must incorporate the corrective value estimated by this equation into the measured value to achieve this.

2. THE EXPERIMENT AND METHODOLOGY

The total heat flux, including radiation and convection, is measured using an unshielded surface heat flux sensor (HF_{us}). This measurement includes radiation-induced errors. As previously mentioned, these errors cannot be mitigated by using a shield. Introducing a shield would exclude radiation fluxes from the total heat flux measured by the sensor, resulting in an even greater error. The difference between the readings from the unshielded surface heat flux sensor (HF_{us}) and the true values (HF_{true}) unveils the radiation-induced errors ($HF_{err.} = HF_{true} - HF_{us}$) that this study aims to evaluate. Our strategy is to find the HF_{true} using an experimental setup, illustrated in Fig. 1. The configuration incorporates two pyranometers, two pyrgeometers, two surface heat flux and temperature sensors, and an air temperature sensor. The four pyranometers and pyrgeometers are labeled "net radiometer" in Fig. 1.The setup allows for independently measuring convection (HF_c) and radiation (HF_r) heat fluxes in a way unaffected by radiation-induced errors. The sum of these two components would provide the accurate total heat flux (HF_{true}). Once HF_{true} becomes available, we plot the error ($HF_{err.} = HF_{true} - HF_{us}$) against incoming long-wave radiation (LWR) and employ linear regression to establish a linear relationship between them ($HF_{err.}$ vs. LWR). This equation can then be used to estimate $HF_{err.}$ by knowing the LWR. The strategy to obtain radiation (HF_r) and convection (HF_c) heat fluxes are explained below, leading to true heat flux as $HF_{true}=HF_r+HF_c$.

Radiation. The net radiomter includes two pyranometers (Apogee SP-510/610-SS) for quantifying shortwave radiation. One of these pyranometers faces upwards, capturing the incoming short-wave radiations received from the sky onto the panel. These spectral shortwave radiation bands that are measured by the pyranometer consist of wavelengths ranging from 370 nm to 2240 nm, accounting for over 97% of the total radiative energy [2]. The second pyranometer faces downward, measuring the outgoing short-wave radiations leaving the

panel's surface. The net radiometer also includes two pyrgeometers (Apogee SL-510/610-SS). These sensors measure the spectral long-wave radiation, consisting of wavelength bands ranging from 5 to 30 micrometers. Similar to the pyranomters, one of these pyrgeometers faces the sky and captures the incoming longwave radiation, while the other pyrgeometer faces the panel and captures the outgoing longwave radiation. This setup allows access to individual radiation components, including downward and upward short-wave and long-wave radiations. This was critical since we did not know which component the radiative error ($HF_{err.}$) is the most sensitive to. We plotted $HF_{err.}$ against all four components, as well as the net radiation (the summation of the downward long-wave and short-wave radiation minus the summation of the upward short-wave and long-wave radiation), to determine which component the $HF_{err.}$ responds to the most.

Convection. The surface temperature and heat flux sensors employed in this study were Hukseflux FHF05 Series. A shielded surface heat flux sensor obtains the heat flux resulting from convective heat transfer as the radiative heat flux is mostly blocked. The shielded sensor's readings yield the convection heat transfer at the location of the shielded sensor, which is less than the convection heat transfer at the location of an unshielded sensor because the shield's shade locally decreases surface temperature. Both shielded and unshielded heat flux sensors could also measure surface temperature. Analyzing the measured data revealed that the difference between the two temperatures increased almost linearly with solar irradiance (incoming short-wave radiation) up to 10 C on very sunny days. Therefore, the convection measured by the shielded sensor is not equal to the convection at the location of the unshielded sensor, as increased surface temperature increases the rate of convection. However, one can correct the convection measured by the shielded sensor to make it applicable to the location of the unshielded sensor. Convective heat flux at the shielded sensor ($HF_{c,s}$) is

$$HF_{c,s} = h \times (T_{p,s} - T_{\infty}) \tag{1}$$

where h is the convection heat transfer coefficient, $T_{p,s}$ is the panel's surface temperature under the shield, and T_{∞} is the air temperature above the panel, measured by an air temperature sensor. Similarly, convective heat flux at the unshielded sensor ($HF_{c,us}$) is

$$HF_{c,us} = h \times (T_{p,us} - T_{\infty}) \tag{2}$$

Hence, the difference between the two of them is

$$\Delta HF_c = h \times (T_{p,us} - T_{p,s}) \tag{3}$$

Solving Eq. 1 for h and substituting it in Eq. 3 yields,

$$\Delta HF_c = \frac{HF_{c,s}}{(T_{p,s} - T_{\infty})} \times (T_{p,us} - T_{p,s}) \tag{4}$$

where ΔHF_c is what one needs to add to the shielded sensor's readings to convert them to the convection at the unshielded sensor; hence, $HF_{c,us}$ can be computed as what the shielded sensor reads plus the corrective value estimated via Eq. 4. In Eq. 4, $HF_{c,s}$ and $T_{p,s}$ is obtained via the shielded heat flux sensor, $(T_{p,us} - T_{p,s})$ is the difference between surface temperatures measured by the unshielded and shielded surface heat flux sensors, and T_{∞} is the air temperature measured by an air temperature sensor.

Radiation-induced error. Thus, the radiation-induced error in measurements of the unshielded heat flux sensor is

$$HF_{err} = HF_{r,net} + HF_{p,s} + \Delta HF_{c,s} - HF_{p,us} \tag{5}$$

where HF_{true}=$HF_{r,net}$+$HF_{p,s}$+$\Delta HF_{c,s}$ is the true value of heat flux, $HF_{r,net}$ is the net radiation heat flux measured by the pyranometers and pyrgeometers and is positive as it enters the panel, $HF_{p,s}$ is the heat flux measured by the shaded panel and is negative as it measures convection heat flux leaving the panel, $\Delta HF_{c,s}$ is the corrective convection term computed via Eq. 4 and is negative, and $HF_{p,us}$ is the heat flux measured by the unshielded sensor, which is positive. HF_{err} is the corrective term.

3. UNCERTAINTY

Table 1 provides uncertainty information of the sensors used in this study.

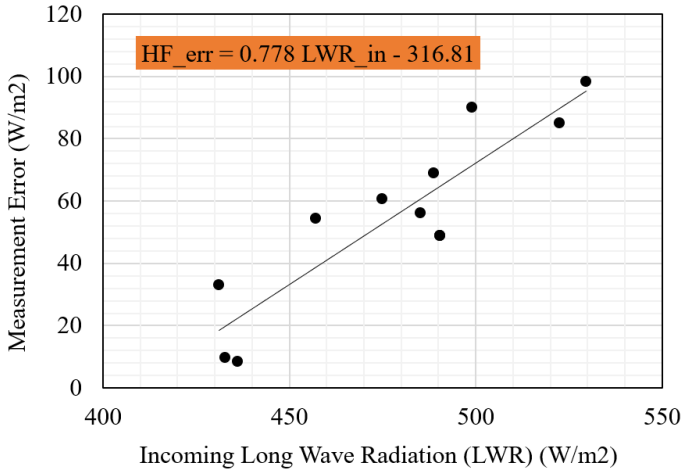

Fig. 2 Linear relationship between radiation errors and solar irradiance.

4. RESULTS AND DISCUSSION

Data collected within three weeks (7 last days of September and the first 14 days of October 2023) was used for this study. Data recorded between 11:00 am and 13:00 pm, where the sun's radiation was perpendicular to the setup, was used to ensure the shielded sensor was not recording radiation flux.

The under-measurement of heat flux ($HF_{err.}$) was calculated on 21 days and plotted versus the incoming short-wave radiation, incoming long-wave radiation, outgoing short-wave radiation, outgoing long-wave radiation, and net radiation. Among all, $HF_{err.}$ appeared to correlate with the incoming long-wave radiation (LWR). This makes sense because the radiation error $HF_{err.}$ is caused by radiation heating the back of the sensor, and most of the heat coming down from the sun to cause this falls within the long-wave range measured by the pyrgeometer. Interestingly, the relationship between the two appeared to be linear, with a coefficient of determination of nearly 0.75, meaning that the line explains more than 75% of the data. According to the curve-fitting, the under-measurement of heat flux ($HF_{err.}$) in W/m^2 can be estimated in terms of incoming long-wave solar radiation (LWR) as

$$HF_{err.} = 0.778 \times LWR - 316.81 \tag{6}$$

We recommend using this equation to correct total surface heat flux data measured by direct contact sensors at PV panel's surfaces.

5. CONCLUSION

There are concerns that large-scale solar farms would become heat islands. This would alter the local climate and affect the surrounding environment. Studies that aim to investigate this potential challenge utilize field measurements. Solar radiation generally interferes with field measurements as it heats the sensors. In general, this problem is addressed using radiation shields, which would not work for heat flux sensors. This study showed that this would lead to an under-measurement of total heat flux at the surface under sunshine. The degree of underestimation exhibits a linear relationship with the downward long-wave radiation (LWR), given by $HF_{err.} = 0.778 \times LWR - 316.81$.

ACKNOWLEDGMENTS

This work was made possible due to a National Science Foundation CAREER grant (award # 2144299).

REFERENCES

[1] A. Vasel and F. Iakovidis, "The effect of wind direction on the performance of solar pv plants," *Energy Conversion and Management*, vol. 153, pp. 455–461, 2017.

[2] H. Kambezidis, "3.02 - the solar resource," in *Comprehensive Renewable Energy* (A. Sayigh, ed.), pp. 27–84, Oxford: Elsevier, 2012.